MECHANICAL PERFORMANCE OF ASPHALT PAVEMENT WITH ORTHOTROPIC UNBOUND GRANULAR SUB-BASE UNDER VEHICLE LOAD

YUANYUAN GAO

School of Civil Engineering and Mechanics, Yanshan University, Qinhuangdao, China

e-mail: gaoyuanyuan2286@ysu.edu.cn

Key Laboratory of Green Construction and Intelligent Maintenance for Civil Engineering of Hebei Province, Yanshan University, Qinhuangdao, China

Hebei High Performance Building Material Technology Innovation Center, Qinhuangdao Municipal Building Materials Group Co. Ltd., Qinhuangdao, China

NKOSILATHI LOVEWELL HLUPO

School of Civil Engineering and Mechanics, Yanshan University, Qinhuangdao, China

e-mail: lovewell1996@gmail.com

QUAN QIAN

Hebei High Performance Building Material Technology Innovation Center, Qinhuangdao Municipal Building Materials Group Co. Ltd., Qinhuangdao, China; e-mail: qhdjcjc@126.com

HONGTAO JIANG

School of Civil Engineering and Mechanics, Yanshan University, Qinhuangdao, China

e-mail: jht0122@stumail.ysu.edu.cn

The nonlinear mechanical response and orthotropy are the main properties of an unbound granular material as a sub-base in an asphalt pavement. To investigate the impact of stress and orthotropy characteristics simultaneously in an unbound granular sub-base, a constitutive relation and a finite model were proposed. The distribution of the sub-base resilience modulus and dynamic response of the pavement under vehicle loads were calculated. The results show an increase in the resilience modulus with a decrease in the orthotropic coefficient. Stress and orthotropy affect the stress distribution near the pavement layer, and vehicle velocity significantly impacts the vertical displacement.

Keywords: asphalt pavement, unbound granular sub-base, stress dependency, orthotropy, mechanical response

1. Introduction

The exponential growth of use of asphalt in the construction worldwide shows its importance to modern transport infrastructure. Understanding the mechanical performance of pavements has become essential for ensuring durability and stability. An unbound granular material is typically used as a base or sub-base of asphalt pavements in China because of its excellent water permeability, diffusion stress and bearing transition performance. Unbound granular materials consist of gravel, crushed stone and fine aggregate (sand) forming a crucial layer that supports and stabilizes the pavement system. The properties of unbound granular materials play a vital role in the overall performance of the asphalt pavement by distributing vehicle loads on the underlying soil. Therefore, the arrangement of particles of different sizes and loading conditions applied to the structures substantially impact the mechanical performance of the unbound granular material. Many researchers have confirmed that the resilience modulus of the unbound granular

material as a pavement layer increases with growth of the stress of the pavement, and the vertical resilience modulus is always larger than the horizontal one (Al-Qadi *et al.*, 2015). In particular, due to the layer-by-layer paving and rolling technology for constructing the road, the unbound granular base in an asphalt pavement exhibits more obvious nonlinear elastic and orthotropic properties. Therefore, the unbound granular properties must be considered when analyzing the mechanical response of the asphalt pavement. Researchers have been exploring the relationship between microstructural properties of the asphalt pavement and its macroscopic behavior by using upscaling techniques to improve the reliability and realism of pavement design, maintenance and performance evaluation (Lackner *et al.*, 2006). Hence the findings of this study will provide valuable insights into the existing knowledge on asphalt pavements ad will contribute to improving pavement designs and maintenance strategies.

In the pavement, the asphalt layer contains a viscoelastic material that exhibits viscous and elastic behavior when subjected to vehicle loads. This behavior provides more accurate calculation results on temperature sensitivity and time-dependent behavior. Additionally, viscoelastic models offer a better and more realistic representation of the mechanical response of the asphalt layer. In particular, Specht *et al.* (2017) used theory of viscoelasticity to investigate the resilient modulus of asphalt mixtures. The results show the difference in stiffness, and the differences substantially affect the resilient modulus response. Many other studies have also demonstrated that considering such viscoelastic behavior during analysis provides greater accuracy when calculating the mechanical response of the asphalt pavement under vehicle loads (Wu *et al.*, 2020). Therefore, the viscoelastic property of the asphalt layer in the pavement is considered in the model proposed in this paper.

The commonly used model for calculating the unbound granular resilience modulus includes the k-θ model, the Uzan model and the NCHRP 1-28A model *et al.* (González *et al.*, 2007). Because of the complexity of determining the unbound granular resilience modulus, researchers have experimented with several models to obtain a more accurate results. The chord formulation has been adopted to describe the resilience modulus of unbound granular materials. It has demonstrated its ability to characterize the mechanical behavior of these materials through calibration using laboratory test results (Aswegen *et al.*, 2015). Bilodeau *et al.* (2016) analyzed factors affecting the unbounded granular base modulus variation. They proposed a new model to calculate the resilient modulus of this base considering the effect of grading, fraction between crushed stones and moisture. Furthermore, Ullah *et al.* (2022) modified the Uzan model by considering the influence of grading, stress level and moisture content. That modification was based on the linear relationship between the resilience modulus and moisture observed in laboratory triaxial test results. Based on the shakedown theory, an elastoplastic constitutive model for unbound granular materials used in pavement applications was established. This model captures the deformation behavior of the material at different stages through the application of repeated loads. The proposed model was validated through a precision unbound material analyzer measuring mixed-size aggregate deformation (Li and Hao, 2020). In calculating the resilience modulus for unbound granular materials, the NCHRP 1-28A model is an effective and widely utilized approach (Sandjak *et al.*, 2020). Its application in assessing the resilience modulus of unbound granular materials has gained prominence due to its reliability and practicality.

To obtain the mechanical performance of an asphalt pavement containing an orthotropic unbound granular base, building a finite element model is one of the most effective methods according to the constitutive relation of the base. During the process of building a finite element model, one of the vital parts is using the finite element method to characterize the constitutive relation of pavement materials. In particular, the resilient modulus of an unbound granular material is a key input parameter in the model. The k-θ model, Uzan model and NCHRP 1-28A model of the resilience modulus are also commonly implemented as crucial information for building the asphalt pavement model containing an unbound granular layer (González *et al.*, 2007).

Cortes *et al.* (2012) adopted a nonlinear elastoplastic material model to capture the unbound granular base performance in a finite-element model. This model satisfies the Hertzian-type stress-dependent stiffness of the unbound granular base and the skeletal softening caused by deviatoric loads that approach failure. The Drucker-Prager model is used to consider the stress dependency of the unbound granular material for building flexible pavement models (Gupta *et al.*, 2015). However, convergence is a challenging issue for the nonlinear model. To deal with this problem, limiting the tensile stress of the unbound granular base to be non-negative and minimum, the value of the unbounded granular resilience modulus is usually adopted (Sahoo and Reddy, 2010). In the asphalt pavement model containing an unbound granular base, changing the stress-dependent constitutive model into a strain-dependent one effectively tackles the convergence difficulties. Then, a new strain tensor updating algorithm can be derived (Li and Guo, 2016). Tension stress can exist in unbound granular materials to a certain degree. Li and Hao (2020) modified the original asphalt pavement model by limiting the maximum tensile stress in the integral point. The calculation results received using this method are closer to the actual working state. According to the literature, most models of the asphalt pavements with an unbound granular base only take into account stress-dependent materials. However, orthotropy is another essential characteristic of the unbound granular layer in simulating the behavior of the asphalt pavement. Therefore, further research is required to provide more precise conclusions regarding the mechanical response of pavements containing the unbound granular layer.

Pavement structures face a multitude of loads during their lifetime, including both static and impact loads. Although a considerable amount of investigation has been conducted on how a static load impacts pavement durability, there is a growing recognition of the importance of considering the effects of impact loads. Vehicle speed significantly affects pavement deformations. For asphalt pavements in China, Assogba *et al.* (2021) reported that the current design code and mechanical analysis procedures are based on laminar elastic theory under static vehicle loads. In this approach, a low traffic volume was primarily analyzes, without considering the actual overload phenomena, vehicle running speed, viscoelastic behavior of the asphalt concrete layer and dynamic characteristics of the load induced by vehicle tires. Therefore, a considerable gap emerges between the proposed design theory and the actual loads on the pavement from moving vehicles. Karamanli *et al.* (2023) found that under moving loads, the structure may exhibit greater stress and displacement compared to static loads. Numerous studies have been conducted considering moving loads to evaluate performance of the structures under various conditions, assessed their structural capacity, and developed more accurate design methodologies for durability and resilience of the structure (Abdelrahman *et al.*, 2021; Esen *et al.*, 2021; Attia *et al.*. 2022; Karamanli *et al.*, 2023). Hence the moving load is a vital factor in the mechanical performance in the pavement analysis.

In this paper, based on the NCHRP 1-28A model, considering both stress dependency and orthotropic properties of an unbound granular material simultaneously, the constitutive relation of the unbound granular sub-base is established. By performing complex derivation, we obtain the consistent tangent modulus of the material. And then, based on the formulation of this consistent tangent modulus, the UMAT material program is compiled to describe properties of the unbound granular sub-base. Furthermore, an asphalt pavement model containing an unbound granular sub-base is constructed. By this model, the resilience modulus distributions in the subbase and the mechanical response of the pavement are received. The influence of stress dependency and orthotropic properties on the mechanical response of the asphalt pavement is analyzed. The proposed method and the results obtained from this paper could provide some suggestions on the design stage of a flexible pavement and asphalt pavement containing an unbound granular layer.

2.   Constitutive relation

Based on the elastic theory and the generalized Hooke's law, the stress-strain relationship at any point can be expressed as (Rao, 2018)

$$\boldsymbol{\sigma} = \mathbf{D}\boldsymbol{\varepsilon} \tag{2.1}$$

where $\boldsymbol{\sigma} = [\sigma_{xx}, \sigma_{yy}, \sigma_{zz}, \sigma_{xy}, \sigma_{yz}, \sigma_{zx}]^{\mathrm{T}}$, $\boldsymbol{\varepsilon} = [\varepsilon_{xx}, \varepsilon_{yy}, \varepsilon_{zz}, \varepsilon_{xy}, \varepsilon_{yz}, \varepsilon_{zx}]^{\mathrm{T}}$, σ_{xx}, σ_{yy}, σ_{zz}, σ_{xy}, σ_{yz} and σ_{zx} are 6 stress components under 3 stress states, respectively. ε_{xx}, ε_{yy}, ε_{zz}, ε_{xy}, ε_{yz} and ε_{zx} are 6 strain components, respectively. Each element in the stiffness matrix $\mathbf{D}$ represents the elastic properties of the material.

In engineering, the elastic modulus E and Poisson's ratio ν are often used to express the stress-strain relationship. Then, the matrix $\mathbf{D}$ can be expressed as (Rao, 2018)

$$\mathbf{D} = \begin{bmatrix} d_{11} & d_{12} & d_{13} & 0 & 0 & 0 \\ d_{21} & d_{22} & d_{23} & 0 & 0 & 0 \\ d_{31} & d_{32} & d_{33} & 0 & 0 & 0 \\ 0 & 0 & 0 & d_{44} & 0 & 0 \\ 0 & 0 & 0 & 0 & d_{55} & 0 \\ 0 & 0 & 0 & 0 & 0 & d_{66} \end{bmatrix} \tag{2.2}$$

In Eq. (2.2)

$$d_{11} = \frac{1 - \nu_{yz}\nu_{yz}}{E_{yy}E_{zz}\Delta} \qquad d_{22} = \frac{1 - \nu_{xz}\nu_{zx}}{E_{xx}E_{zz}\Delta} \qquad d_{33} = \frac{1 - \nu_{xy}\nu_{yx}}{E_{xx}E_{yy}\Delta}$$

$$d_{12} = \frac{\nu_{yx} + \nu_{zx}\nu_{yz}}{E_{yy}E_{zz}\Delta} \qquad d_{21} = \frac{\nu_{xy} + \nu_{xz}\nu_{zy}}{E_{xx}E_{zz}\Delta} \qquad d_{23} = \frac{\nu_{zy} + \nu_{xy}\nu_{zx}}{E_{xx}E_{zz}\Delta}$$

$$d_{32} = \frac{\nu_{yz} + \nu_{yx}\nu_{xz}}{E_{xx}E_{yy}\Delta} \qquad d_{31} = \frac{\nu_{xz} + \nu_{xy}\nu_{yz}}{E_{xx}E_{yy}\Delta} \qquad d_{13} = \frac{\nu_{zx} + \nu_{yx}\nu_{zy}}{E_{yy}E_{zz}\Delta}$$

$$d_{44} = \frac{E_{xx}}{2(1 + \nu_{xy})} \qquad d_{55} = \frac{E_{yy}}{2(1 + \nu_{yz})} \qquad d_{66} = \frac{E_{zz}}{2(1 + \nu_{zx})}$$

$$\Delta = \frac{1 - \nu_{xy}\nu_{yx} - \nu_{yz}\nu_{zy} - \nu_{zx}\nu_{xz} - 2\nu_{xy}\nu_{yz}\nu_{zx}}{E_{xx}E_{yy}E_{zz}}$$

where E_{xx}, E_{yy}, E_{zz} are the elastic modulus in the x, y, z directions, respectively, and G_{yz}, G_{zx}, G_{xy} are the shear moduli in the yz, zx, xy planes, respectively. ν_{yz}, ν_{zx} and ν_{xy} are Poisson's ratios in the x, y and z directions, respectively.

Because Poisson's ratio ν in the x, y and z direction has a little difference, Poisson's ratio is regarded as isotropic, and only an orthotropic elastic modulus E is considered in this paper. In the unbound granular layer of an asphalt pavement, the elastic modulus in the vertical direction is usually larger than that in the horizontal direction. If it is assumed that $E_{xx} = n_1 E_{zz}$, $E_{yy} = n_2 E_{zz}$, the values of n_1 and n_2 are greater than 0 and less than 1. Then Eq. (2.2) can be modified as (Rao, 2018)

$$\mathbf{D} = \begin{bmatrix} \frac{1-\nu}{(1-2\nu)(1+\nu)}\frac{1}{n_1}E_{zz} & \frac{1-\nu}{(1-2\nu)(1+\nu)}\frac{1}{n_1}E_{zz} & \frac{1-\nu}{(1-2\nu)(1+\nu)}\frac{1}{n_1}E_{zz} & 0 & 0 & 0 \\ \frac{1-\nu}{(1-2\nu)(1+\nu)}\frac{1}{n_2}E_{zz} & \frac{1-\nu}{(1-2\nu)(1+\nu)}\frac{1}{n_2}E_{zz} & \frac{1-\nu}{(1-2\nu)(1+\nu)}\frac{1}{n_2}E_{zz} & 0 & 0 & 0 \\ \frac{1-\nu}{(1-2\nu)(1+\nu)}E_{zz} & \frac{1-\nu}{(1-2\nu)(1+\nu)}E_{zz} & \frac{1-\nu}{(1-2\nu)(1+\nu)}E_{zz} & 0 & 0 & 0 \\ 0 & 0 & 0 & \frac{1}{n_1}\frac{E_{zz}}{2(1+\nu)} & 0 & 0 \\ 0 & 0 & 0 & 0 & \frac{1}{n_2}\frac{E_{zz}}{2(1+\nu)} & 0 \\ 0 & 0 & 0 & 0 & 0 & \frac{E_{zz}}{2(1+\nu)} \end{bmatrix} \tag{2.3}$$

Since the stiffness matrix of isotropic elastic materials can be expressed as

$$\mathbf{K} = \begin{bmatrix} \frac{1-\nu}{(1-2\nu)(1+\nu)}E_{zz} & \frac{1-\nu}{(1-2\nu)(1+\nu)}E_{zz} & \frac{1-\nu}{(1-2\nu)(1+\nu)}E_{zz} & 0 & 0 & 0 \\ \frac{1-\nu}{(1-2\nu)(1+\nu)}E_{zz} & \frac{1-\nu}{(1-2\nu)(1+\nu)}E_{zz} & \frac{1-\nu}{(1-2\nu)(1+\nu)}E_{zz} & 0 & 0 & 0 \\ \frac{1-\nu}{(1-2\nu)(1+\nu)}E_{zz} & \frac{1-\nu}{(1-2\nu)(1+\nu)}E_{zz} & \frac{1-\nu}{(1-2\nu)(1+\nu)}E_{zz} & 0 & 0 & 0 \\ 0 & 0 & 0 & \frac{E_{zz}}{2(1+\nu)} & 0 & 0 \\ 0 & 0 & 0 & 0 & \frac{E_{zz}}{2(1+\nu)} & 0 \\ 0 & 0 & 0 & 0 & 0 & \frac{E_{zz}}{2(1+\nu)} \end{bmatrix} \tag{2.4}$$

therefore, the stiffness matrix can be expressed as

$$\mathbf{D} = \mathbf{HK} \tag{2.5}$$

where $\mathbf{H}$ is a diagonal matrix presented as

$$\mathbf{H} = \begin{bmatrix} \frac{1}{n_1} & 0 & 0 & 0 & 0 & 0 \\ 0 & \frac{1}{n_2} & 0 & 0 & 0 & 0 \\ 0 & 0 & 1 & 0 & 0 & 0 \\ 0 & 0 & 0 & \frac{1}{n_1} & 0 & 0 \\ 0 & 0 & 0 & 0 & \frac{1}{n_2} & 0 \\ 0 & 0 & 0 & 0 & 0 & 1 \end{bmatrix} \tag{2.6}$$

Seed *et al.* (1967) introduced the concept of resilience modulus while investigating the relationship between the resilience characteristic of a subgrade soil and fatigue damage of an asphalt pavement. The resilience modulus is the ratio of the maximal deviator stress to the maximal resilience strain after deformation is stabilized under a repeated load. It can be expressed as

$$M_r = \frac{\sigma_d}{\varepsilon_r} \tag{2.7}$$

where M_r is the resilience modulus. $\sigma_d = \sigma_1 - \sigma_3$ is the resilience stress (deviator stress). σ_1 and σ_3 are the maximun and minimun stress, respectively, and ε_r is the maximum resilience strain.

The NCHRP 1-28A model provides a calculation formula for the dynamic resilience modulus, and it can be expressed as (Sandjak *et al.*, 2020)

$$M_r(\theta, \tau_{oct}) = k_1 P_a \Big(\frac{\theta}{P_a}\Big)^{k_2} \Big(\frac{\tau_{oct}}{P_a} + 1\Big)^{k_3} \tag{2.8}$$

where M_r is the resilience modulus, θ is the volume stress and τ_{oct} is the shear stress $\tau_{oct} = \sqrt{(\sigma_1 - \sigma_2)^2 + (\sigma_2 - \sigma_3)^2 + (\sigma_3 - \sigma_1)^2}/3$. P_a is atmospheric pressure, and it is generally $100\,\mathrm{kPa}$. k_1, k_2 and k_3 are material constants coming from the test data.

Considering the nonlinear stress dependency of the unbound granular sub-base, the modulus E_{zz} in Eq. (2.3) can be replaced by the dynamic resilience modulus calculated by the NCHRP 1-28A model.

3. Numerical model

3.1. Model of the asphalt pavement containing an unbound granular layer

An asphalt model is established using the finite element software ABAQUS to analyze the effect of stress dependency and orthotropic properties of the unbound granular layer on the dynamic response of the asphalt pavement. To balance the accuracy and time consumption, the

model size is $6\,\mathrm{m}\times6\,\mathrm{m}\times3.76\,\mathrm{m}$. The pavement structure and boundary of the model are adopted the same as in the literature (Yan and Wang, 2016), and the same material parameters of the asphalt layer given in the literature (Yan and Wang, 2016) are also used in this paper. The contact area between the vehicle and the pavement surface is simplified as a rectangle, and the size is $0.184\,\mathrm{m}\times0.192\,\mathrm{m}\times2$. It assumes that the vehicle load is located in this area. The distance between the two wheels is $0.225\,\mathrm{m}$, and the contact pressure is $P = 700\,\mathrm{kPa}$. Figure 1 is a sketch map of the vehicle load. Because of symmetry, a half model is selected to analyze. To capture the
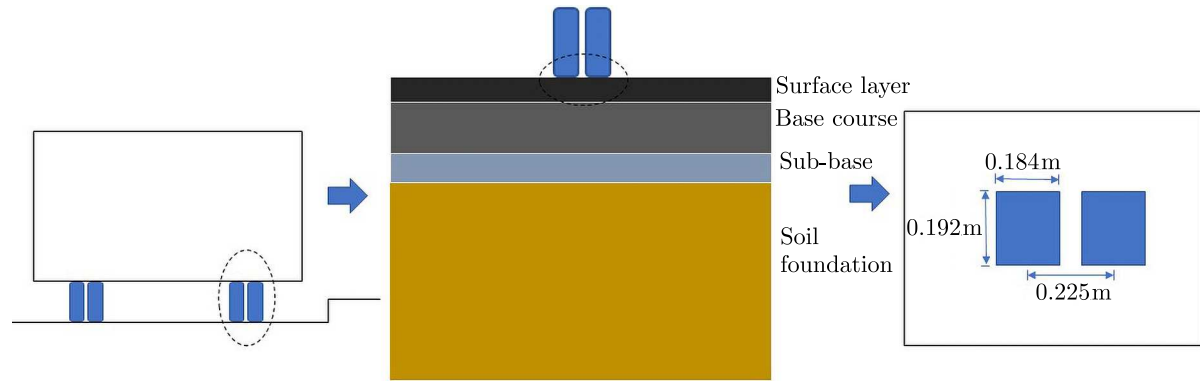
Fig. 1. Vehicle load sketch map

pavement behavior caused by a vehicle driving on the road, the loaded track starts at $1.464\,\mathrm{m}$ from one end of the model, the track length is $3.072\,\mathrm{m}$, and the vehicle speed is $90\,\mathrm{km/h}$. Figure 2 presents the asphalt model containing an unbound granular sub-base and the vehicle track. The details of geometry and material parameters are shown in Table 1. In this model shown in Fig. 2,
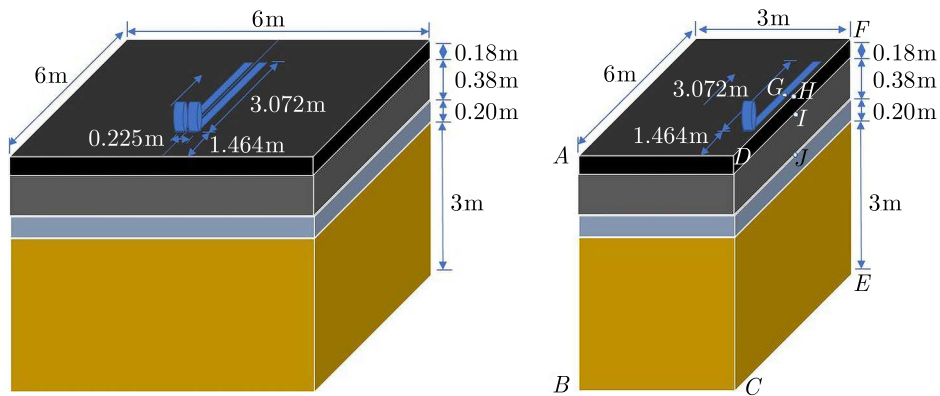
Fig. 2. Asphalt pavement containing an unbound granular sub-base

the boundary at the bottom is fixed, the displacement in the normal direction and rotation in the two tangential directions in the symmetry plane are constrained, and the normal displacement in the plane along the long edge and the two planes along the short edge of the model is 0. The asphalt pavement model is meshed by C3D8R element, which is an 8-node linear brick, reduced integration and hourglass control element. Adopting this element reduces the calculation time and avoids the shear-locking phenomenon to obtain relatively accurate results. The geometry, boundary conditions and mesh of the pavement model are shown in Figs. 3a-3c.

ABAQUS is an effective tool for solving dynamic problems. Because the growth of strain is a function of strain and the strain rates are lower than 10 units per second in this model, the Dynamic Implicit solver is adopted to calculate the dynamic response of this model. This solver uses the Newton-Raphson numerical algorithm and Newmark-β method to solve dynamic equilibrium equations, and the stiffness matrix is updated in each increment. This method is
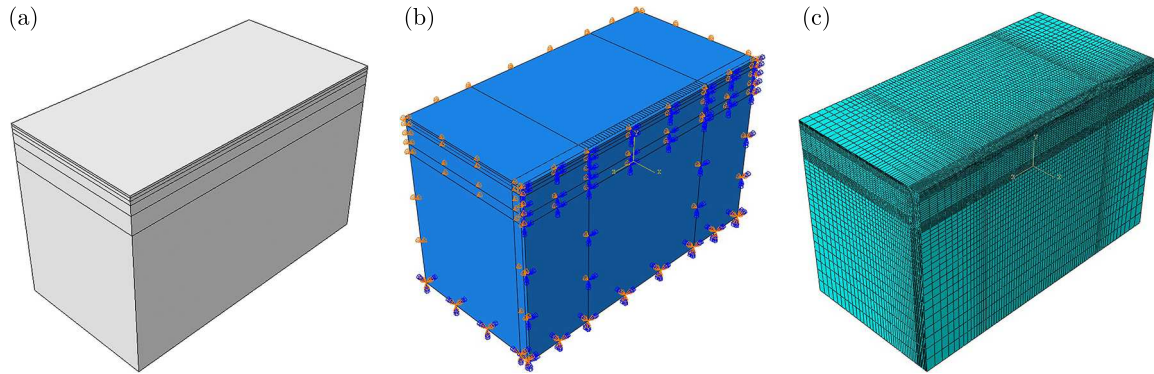
Fig. 3. Finite element model of the asphalt pavement: (a) geometry, (b) boundary conditions, (c) meshing

Table 1. Pavement geometry and material parameters

Pavement structure		Material name	Thickness [m]	Modulus [MPa]	Poisson's ratio	Density [kg/m³]
Asphalt layer	Upper layer	AC-13C	0.040	Same with literature (Yan and Wang, 2016)	0.3	2300
	Middle layer	Sup-20	0.060	Same with literature (Yan and Wang, 2016)	0.3	2300
	Lower layer	Sup-25	0.080	Same with literature (Yan and Wang, 2016)	0.3	2300
Base course		Cement stabilized macadam	0.380	15000	0.2	2300
Sub-base		Unbound granular	0.200	$k_1 = 3170$, $k_2 = 0.06$, $k_3 = 0.43$ (Wang *et al.*, 2022)	0.3	2100
Soil foundation		Compacted soil	3.000	45	0.4	1850

unconditionally stable, for any initial assumption of Δt, the solution converges, and there is no mathematical time limit for the solution. In this model, the vehicle travelling time is 0.11776 s, and the increment size is 0.00256 s.

3.2. Tangent stiffness matrix

Newton's iterative method is an effective tool for solving nonlinear finite element models, and obtaining the tangent stiffness matrix is necessary for this method. The tangent stiffness modulus is a matrix that describes the relationship between stress differential and strain differential according to the current state of variables (stress, strain, etc.). Finding the tangent stiffness modulus generally starts from the constitutive relation of this material. Due to the resilience modulus being a function of stress and the orthotropic constitutive equations, it enhances difficulties of the formula derivation. This paper presents a new feature for obtaining the tangent stiffness matrix considering the stress dependency and orthotropy of the constitutive relationship.

The linear elastic constitutive equation in a tensor form can be expressed as

$$\boldsymbol{\sigma} = \frac{E}{1+\nu}\boldsymbol{\varepsilon} + \lambda \operatorname{tr}(\boldsymbol{\varepsilon})\mathbf{1} \tag{3.1}$$

where $\boldsymbol{\sigma} = [\sigma_{xx}, \sigma_{yy}, \sigma_{zz}, \sigma_{xy}, \sigma_{yz}, \sigma_{zx}]^{\mathrm{T}}$, $\boldsymbol{\varepsilon} = [\varepsilon_{xx}, \varepsilon_{yy}, \varepsilon_{zz}, \varepsilon_{xy}, \varepsilon_{yz}, \varepsilon_{zx}]^{\mathrm{T}}$, $\mathbf{1} = [1,1,1,0,0,0]^{\mathrm{T}}$, $\operatorname{tr}(\boldsymbol{\varepsilon})$ is the volume strain.

Similar to the linear elastic constitutive relation, based on Eq. (3.1), the nonlinear elastic constitutive equation of the unbound granular sub-base can be rewritten as

$$\boldsymbol{\sigma} = \frac{M_r}{1+\nu}\boldsymbol{\varepsilon} + \lambda \operatorname{tr}(\boldsymbol{\varepsilon})\mathbf{1} \tag{3.2}$$

As known in Eq. (2.8), M_r is a function of the volume stress θ and shear stress τ_{oct}.

If orthotropy of the unbound granular sub-base is considered, based on constitutive relation Eq. (2.5), equation (3.2) can be modified as

$$\widetilde{\boldsymbol{\sigma}} = \frac{M_r}{1+\nu}\overline{\mathbf{H}}\boldsymbol{\varepsilon} + \lambda \operatorname{tr}(\boldsymbol{\varepsilon})\overline{\mathbf{H}}\mathbf{1} \tag{3.3}$$

According to the relationship between Eqs. (3.2) and (3.3), one can obtain

$$\widetilde{\boldsymbol{\sigma}} = \overline{\mathbf{H}}\boldsymbol{\sigma} \tag{3.4}$$

where $\overline{\mathbf{H}}$ is a tensor form of the matrix $\mathbf{H}$.

According to equation (3.3), the consistent tangent modulus can be expressed as

$$\frac{\partial \widetilde{\boldsymbol{\sigma}}}{\partial \boldsymbol{\varepsilon}} = \frac{\partial \widetilde{\boldsymbol{\sigma}}}{\partial \boldsymbol{\sigma}}\frac{\partial \boldsymbol{\sigma}}{\partial \boldsymbol{\varepsilon}} \tag{3.5}$$

where

$$\frac{\partial \widetilde{\boldsymbol{\sigma}}}{\partial \boldsymbol{\sigma}} = \overline{\mathbf{H}} \tag{3.6}$$

Therefore, if $\partial \boldsymbol{\sigma}/\partial \boldsymbol{\varepsilon}$ is obtained, the consistent tangent modulus $\partial \widetilde{\boldsymbol{\sigma}}/\partial \boldsymbol{\varepsilon}$ will also be received.

To simplify the process of formula derivation, let

$$B(\theta, \tau_{oct}) = \frac{M_r(\theta, \tau_{oct})}{1+\nu} = kP_a\left(\frac{\theta}{P_a}\right)^{k_2}\left(\frac{\tau_{oct}}{P_a} + 1\right)^{k_3} \tag{3.7}$$

where $k = k_1/(1+\nu)$.

And then, Eq. (3.2) can be rewritten as

$$\boldsymbol{\sigma} = B(\theta, \tau_{oct})[\boldsymbol{\varepsilon} + \alpha \operatorname{tr}(\boldsymbol{\varepsilon})\mathbf{1}] \tag{3.8}$$

where $\alpha = \nu/(1-2\nu)$, and the incremental relationship of Eq. (3.8) can be expressed as follows

$$\begin{aligned} \Delta\boldsymbol{\sigma}_{n+1} &= B(\theta, \tau_{oct})_{n+1}[\Delta\boldsymbol{\varepsilon}_{n+1} + \alpha \operatorname{tr}(\Delta\boldsymbol{\varepsilon}_{n+1})\mathbf{1}] \\ B(\theta, \tau_{oct})_{n+1} &= kP_a\left(\frac{\theta_n}{P_a}\right)^{k_2}\left[\frac{(\tau_{oct})_n}{P_a} + 1\right]^{k_3} \end{aligned} \tag{3.9}$$

where the subscript $n+1$ represents the calculation result under the current incremental step and n represents the calculation result of the previous step.

Based on Eq. (3.8), the volume stress and deviatoric stress are expressed as

$$\operatorname{tr}(\boldsymbol{\sigma}) = \overline{\alpha}B(\theta, \tau_{oct})\operatorname{tr}(\boldsymbol{\varepsilon}) \qquad \overline{\boldsymbol{\sigma}} = B(\theta, \tau_{oct})\overline{\boldsymbol{\varepsilon}} \tag{3.10}$$

where $\overline{\alpha} = 3\alpha + 1 = (1 + \nu)/(1 - 2\nu)$ and $\overline{\varepsilon}$ is the deviatoric stress tensor, $\overline{\varepsilon} = \varepsilon - \text{tr}(\varepsilon)\mathbf{1}/3$.

After a series of formula deductions and simplifications, $\partial\boldsymbol{\sigma}/\partial\boldsymbol{\varepsilon}$ can be gained as

$$\frac{\partial\boldsymbol{\sigma}}{\partial\boldsymbol{\varepsilon}} = B(\mathbf{I} + \alpha\mathbf{1} \otimes \mathbf{1}) + \left(\frac{1}{3}\overline{\alpha}\varepsilon\mathbf{1} + \overline{\varepsilon}\right) \otimes \nabla_\varepsilon B = B(\mathbf{I} + \alpha\mathbf{1} \otimes \mathbf{1} + m\mathbf{L}) \tag{3.11}$$

where

$$\mathbf{L} = \frac{\overline{\alpha}k_2(\tau_{oct} + P_a)}{3}\mathbf{1} \otimes \mathbf{1} + \frac{\overline{\alpha}k_2(\tau_{oct} + P_a)}{\text{tr}(\boldsymbol{\sigma})}\overline{\boldsymbol{\sigma}} \otimes \mathbf{1} + \frac{\text{tr}(\boldsymbol{\sigma})k_3}{9\tau_{oct}}\mathbf{1} \otimes \overline{\boldsymbol{\sigma}} + \frac{k_3}{3\tau_{oct}}\overline{\boldsymbol{\sigma}} \otimes \overline{\boldsymbol{\sigma}}$$

Therefore, the consistent tangent modulus $\partial\widetilde{\boldsymbol{\sigma}}/\partial\boldsymbol{\varepsilon}$ can be expressed as

$$\frac{\partial\widetilde{\boldsymbol{\sigma}}}{\partial\boldsymbol{\varepsilon}} = \frac{\partial\widetilde{\boldsymbol{\sigma}}}{\partial\boldsymbol{\sigma}}\frac{\partial\boldsymbol{\sigma}}{\partial\boldsymbol{\varepsilon}} = B\overline{\mathbf{H}}(\boldsymbol{I} + f_1\mathbf{1} \otimes \mathbf{1} + f_2\overline{\boldsymbol{\sigma}} \otimes \mathbf{1} + f_3\mathbf{1} \otimes \overline{\boldsymbol{\sigma}} + f_4\overline{\boldsymbol{\sigma}} \otimes \overline{\boldsymbol{\sigma}}) \tag{3.12}$$

where

$$f_1 = \alpha + m\frac{\overline{\alpha}k_2(\tau_{oct} + P_a)}{3} \qquad f_2 = m\frac{\overline{\alpha}k_2(\tau_{oct} + P_a)}{\text{tr}(\boldsymbol{\sigma})}$$

$$f_3 = m\frac{\text{tr}(\boldsymbol{\sigma})k_3}{9\tau_{oct}} \qquad f_4 = m\frac{k_3}{3\tau_{oct}}$$

Based on the formulation of the consistent tangent modulus $\partial\widetilde{\boldsymbol{\sigma}}/\partial\boldsymbol{\varepsilon}$, the UMAT program of the orthotropic nonlinearly elastic material is compiled. And then, by limiting the allowable maximum tensile stress, the mechanical response of the asphalt pavement model can be obtained.

4. Results and discussion

To analyze the influence of the orthotropic degree of the unbound granular sub-base on the mechanical response of the asphalt pavement based on the proposed procedure, the resilience modulus distribution in the unbound granular sub-base and the stress and displacement of the asphalt pavement are calculated. The results are shown in Figs, 4-8.

Because the resilient modulus distribution in the unbound granular sub-base is almost symmetrical on both sides of the wheel, so Figs. 4a-4d present the contour maps of the resilient modulus distribution in the unbound granular sub-base in the symmetry plane (plane CDFE) of the model with different orthotropic coefficients after the vehicle running at 0.00512 s. Compared with Figs. 4a-4d, the resilience modulus in each figure almost decreases from the top to the bottom of this layer. However, the gradients of the resilience modulus are different with different orthotropic coefficients. In Fig. 4a, the orthotropic coefficient $n_1 = n_2 = 1$, which means the material is isotropic in the unbound granular sub-base, and the maximum and minimum values of the resilience modulus are 301.37 MPa and 275.652 Mpa, respectively. The maximum values of the resilience modulus in Figs. 4b and 4c all emerge directly below the wheel center and the top of the sub-base layer. The minimum values of the resilience modulus in Figs. 4b and 4c all emerge directly below the wheel center and the bottom of this layer. The maximum and minimum values are approximately 326 MPa and 250 MPa, respectively, larger than the gradients shown in Fig. 4a. It means that the orthotropic coefficients in the transverse and longitudinal directions have almost the same effect on the distribution of the resilience modulus. Furthermore, when the unbound granular sub-base is transversaly isotropic $n_1 = n_2 = 0.2$, the difference in the resilience modulus value between the top and bottom of the layer is larger than those shown in Figs. 4a-4c. The maximum and minimum values are 350 MPa and 250 MPA. Therefore, the resilience modulus gradient increases as the orthotropic coefficients decrease in the unbound granular sub-base layer.
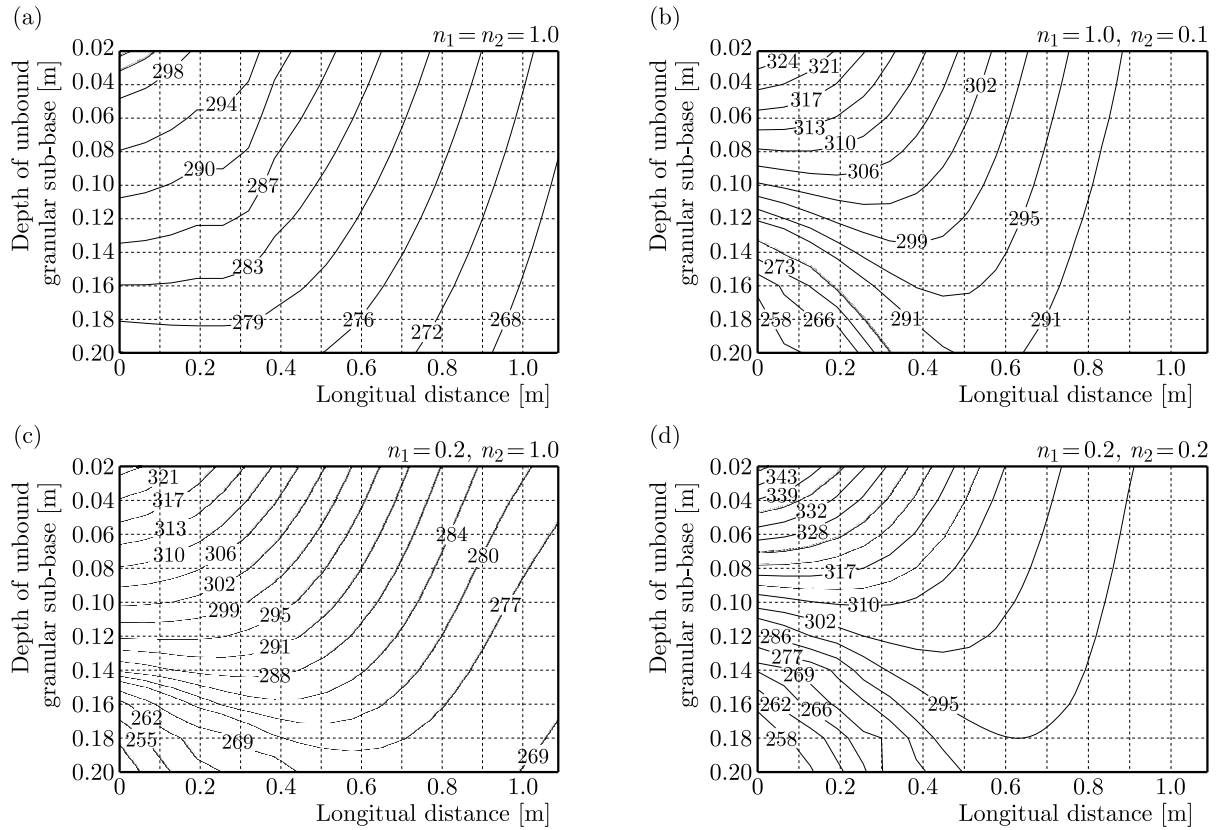
Fig. 4. Distribution of the resilience modulus of the unbound granular material with different orthotropic coefficients

The resilience modulus distribution changing in the unbound granular sub-base causes variation of the stress distribution in this layer. Even this affects the displacement and stress in other layers of this asphalt pavement model. Therefore, in this paper, the influence of the orthotropic coefficient in the sub-base on the mechanical response of the pavement is analyzed by comparing the tensile stress at the bottom of the asphalt layer and base and the displacement on the pavement surface. At the middle of the asphalt layer bottom (point I in the model), the transverse and longitudinal stresses generated by the vehicle driving load are calculated, and the results are shown in Figs. 5a and 5b.
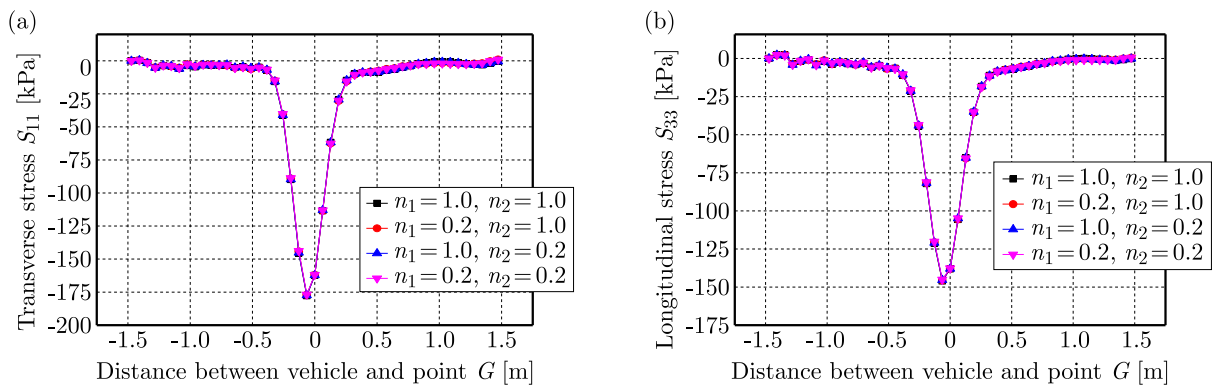
Fig. 5. Calculation results of transverse and longitudinal stresses (at point I) at the bottom of the asphalt pavement

Figures 6a and 6b present the variation of the transverse and longitudinal stress at the top center of the base (point J in the model) under a vehicle load. The pavement surface displacement variation (point G and point H in this model) is shown in Figs. 7a and 7b.
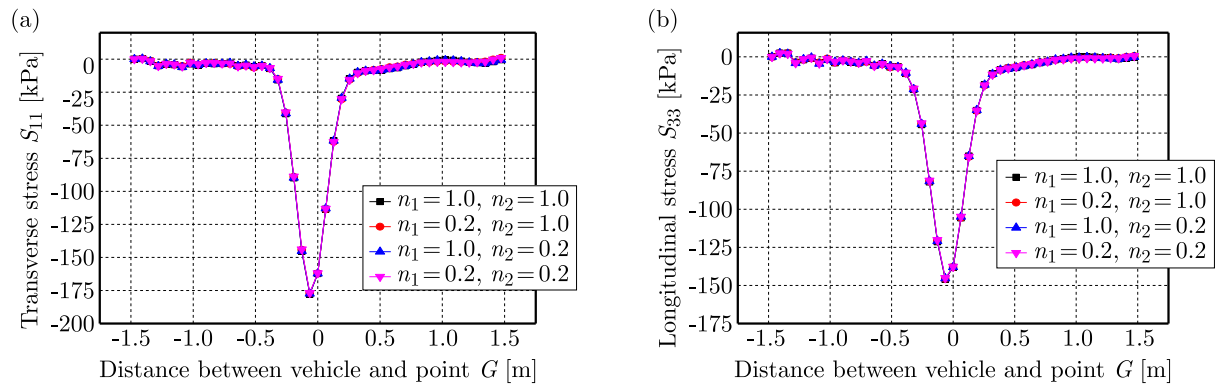
Fig. 6. Calculation results of transverse and longitudinal stresses (at point J) at the bottom of the base layer
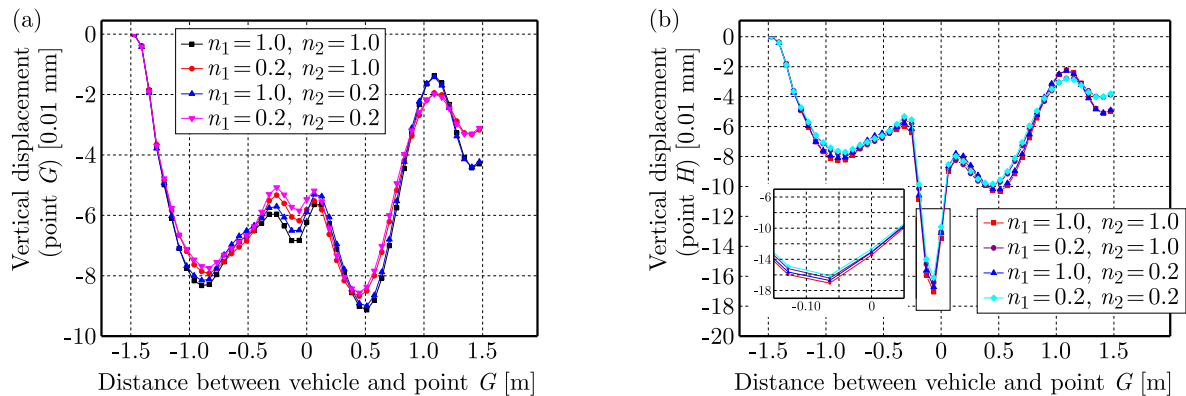
Fig. 7. Calculation results of the vertical displacement at points G and H in the model

The calculation results shown in Figs. 5a and 5b illustrate that the orthotropic coefficient of the sub-base has little effect on the variation of both transverse and longitudinal stresses at the bottom of the asphalt layer. The possible reason is that the unbound granular sub-base is relatively far from the asphalt layer. Therefore, the distribution of the resilience modulus in the sub-base slightly affects the mechanical response in the asphalt layer.

In Fig 6a, the transverse stress in the base sharply decreases with the longitudinal resilience modulus decreasing. In contrast, in Fig. 6b, the longitudinal resilience modulus reduction in the unbounded granular sub-base enlarges the longitudinal stress in the base. On one hand, compared with the asphalt layer, the base is closer to the sub-base, which causes the resilience modulus distribution in the unbounded granular sub-base to considerably affect the stress distribution in the base. On the other hand, the distribution of stress and resilience modulus always has the same variation tendency, which is consistent with our basic understanding. Therefore, to reduce the early damage and extend the pavement service life, the modulus of any layer or one direction of the modulus in the pavement can be manually adjusted through the pavement materials selection to make the stress distribution in the pavement more reasonable.

Figure 7 indicates that the vertical displacement at points G and H of the model decreases as the orthotropic coefficient decreases in the unbound granular sub-base. Compared with the longitudinal orthotropic coefficient, the transverse orthotropic coefficient contributes more to the displacement of the pavement. The vertical displacement of the asphalt pavement is one

of the essential indexes used in evaluating quality of the pavement. In the case of ignoring the orthotropic property, the displacement calculation results are always larger than the real values because the vertical resilience modulus of the unbounded granular base is always larger than its horizontal resilience modulus. Therefore, the results will affect the prediction and assessment of service conditions of the asphalt pavement to a certain extent.

Considering the velocity of a moving vehicle, vertical displacements at point H in this model are calculated with orthotropic coefficients $n_1 = n_2 = 1$ and $n_1 = n_2 = 0.5$. The results are presented in Figs. 8a and 8b, respectively. The velocity of the moving vehicle significantly affects the magnitude and variation of the vertical displacement of the asphalt pavement. It means that the velocity of a moving vehicle is one of the considerable factors for pavement design and assessment. Because of the paper length limitation, the stress distribution in this model with different velocities of a moving vehicle will be presented in the future work.
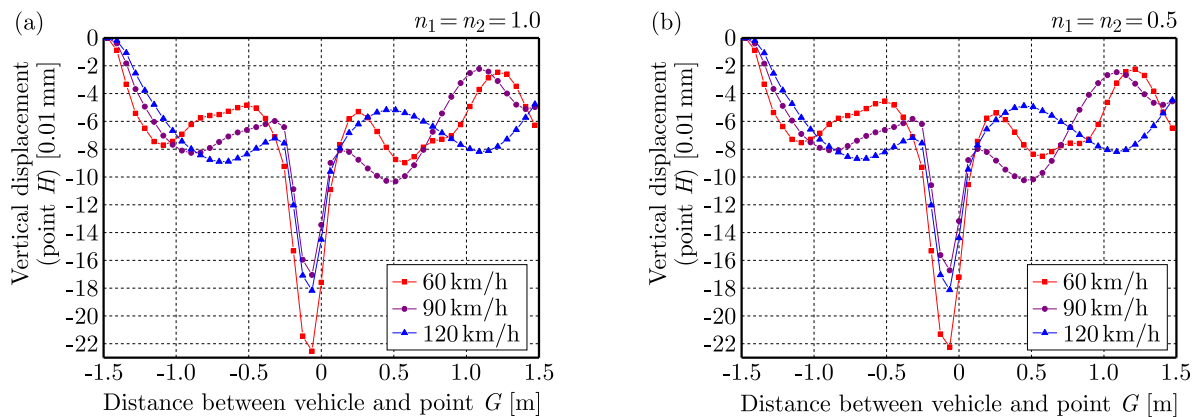
Fig. 8. Calculation results of vertical displacement at points G in the model considering different vehicle speeds

5. Conclusion

Considering the orthotropic and stress dependencies of the unbounded granular base, the NCHRP 1-28A model is adopted to calculate the resilience modulus in this paper. Based on the constitutive relation of an unbound granular sub-base, the consistent tangent modulus is derived for establishing the finite element model of the asphalt pavement containing an unbound granular sub-base. In this pavement model, the asphalt layer is assumed to be a viscoelastic material, and the base is considered elastic. The distribution of the resilience modulus in the sub-base and the mechanical response of the pavement are calculated. Some conclusions can be drawn from the results.

- The stress dependency and orthotropy are fundamental properties of the unbound granular sub-base. As the orthotropic coefficient decreases, the gradient of the resilience modulus increases.
- Orthotropy of the unbound granular sub-base affects the mechanical response of pavement, especially the mechanical response of the layers closer to the sub-base.
- Vertical displacement is an essential index for evaluating the overall stiffness of the pavement during the procedure of pavement performance evaluation and pavement design. The vertical displacement of the pavement is affected to some extent by considering the orthotropy of the unbound granular sub-base. Therefore, it again illustrates the necessity of treating the unbound granular layer as an orthotropic material in the calculation model.

- The velocity of a moving vehicle on the asphalt pavement is also a considerable factor influencing vertical displacement of the pavement. It is necessary to consider it in the pavement design and evaluation.

References

1. ABDELRAHMAN A.A., ESEN I., ÖZARPA C., ELTAHER M.A., 2021, Dynamics of perforated nanobeams subject to moving mass using the nonlocal strain gradient theory, *Applied Mathematical Modelling*, **96**, 215-235

2. AL-QADI I., WANG H., TUTUMLUER E., 2015, Dynamic analysis of thin asphalt pavements by using cross-anisotropic stress-dependent properties for granular layer, *Transportation Research Record: Journal of the Transportation Research Board*, **2154**, 156-163

3. ASSOGBA O.C., TAN Y., SUN Z., LUSHINGA N., BIN Z., 2021, Effect of vehicle speed and overload on dynamic response of semi-rigid base asphalt pavement, *Road Materials and Pavement Design*, **22**, 3, 572-602

4. ASWEGEN E., STEYN W., THEYSE H., 2015, Development of a saturation and stress-dependent chord modulus model for unbound granular material, *Journal of the South African Institution of Civil Engineering*, **57**, 2, 8-21

5. ATTIA M.A., MELAIBARI A., SHANAB R.A., ELTAHER M.A., 2022, Dynamic analysis of sigmoid bidirectional FG microbeams under moving load and thermal load: Analytical Laplace solution, *Mathematics*, **10**, 24, 4797

6. BILODEAU J.P., PLAMONDON C.O., DORÉ G., 2016, Estimation of resilient modulus of unbound granular materials used as pavement base: combined effect of grain-size distribution and aggregate source frictional properties, *Materials and Structures*, **49**, 4363–4373

7. CORTES D.D., SHIN H., SANTAMARINA J.C., 2012, Numerical simulation of inverted pavement systems, *Journal of Transportation Engineering*, **138**, 12, 1507-1519

8. ESEN I., ELTAHER M.A., ABDELRAHMAN A.A., 2023, Vibration response of symmetric and sigmoid functionally graded beam rested on elastic foundation under moving point mass, *Mechanics Based Design of Structures and Machines*, **51**, 5, 2607-2631

9. GONZÁLEZ A., SALEH M., ALI A., 2007, Evaluating nonlinear elastic models for unbound granular materials in accelerated testing facility, *Transportation Research Record: Journal of the Transportation Research Board*, **1990**, 1, 141-149

10. GUPTA A., KUMAR P., RASTOGI R., 2015, Critical pavement response analysis of low-volume pavements considering nonlinear behavior of materials, *Transportation Research Record: Journal of the Transportation Research Board*, **2474**, 1, 3-11

11. KARAMANLI A., ELTAHER M.A., THAI S., VO T.P., 2023. Transient dynamics of 2D-FG porous microplates under moving loads using higher order finite element model, *Engineering Structures*, **278**, 115566

12. LACKNER R., BLAB R., EBERHARDSTEINER J., MANG H.A., 2006, Characterization and multiscale modeling of asphalt-recent developments in upscaling of viscous and strength properties, *III European Conference on Computational Mechanics: Solids, Structures and Coupled Problems in Engineering*, Springer, Netherlands

13. LI N., MA B., WANG H., SUN W., 2020, Development of elasto-plastic constitutive model for unbound granular materials under repeated loads, *Transportation Geotechnics*, **23**, 100347

14. LI S., GUO Z., 2016, Applicability and verification of unbound granular material elastic deformation constitutive model, *Journal of Tongji University: Natural Science*, **44**, 8, 1227-1233

15. LI S., HAO P., 2020, Stress dependent and redistribution behaviour of unbound granular material, *International Journal of Pavement Engineering*, **21**, 3, 347-356

16. RAO S.S., 2018, *The Finite Element Method in Engineering*, 6th Ed., Elsevier

17. SAHOO U.C., REDDY K.S., 2010, Effect of nonlinearity in granular layer on critical pavement responses of low volume roads, *International Journal of Pavement Research and Technology*, **3**, 6, 320-325

18. SANDJAK K., OUANANI M., TILIOUINE B., 2020, Experimental characterisation and numerical modelling of the resilient behaviour of unbound granular materials for roads, *Journal of Building Materials and Structures*, **7**, 2, 159-177

19. SEED H.B., MITRY F.G., MONISMITH C.L., CHAN C.K., 1967, Prediction of flexible pavement deflections from laboratory repeated-load tests, NCHRP report

20. SPECHT L.P., BABADOPULOS L.F.D.A.L., DI BENEDETTO H., SAUZAT C., SOARES J.B., 2017, Application of the theory of viscoelasticity to evaluate the resilient modulus test in asphalt mixes, *Construction and Building Materials*, **149**, 15, 648-658

21. ULLAH S., JAMAL A., ALMOSHAOGEH M., ALHARBI F., HUSSAIN J., 2022, Investigation of resilience characteristics of unbound granular materials for sustainable pavements, *Sustainability*, **14**, 6874

22. WANG M., YU Q., XIAO Y., LI W., 2022, Resilient modulus behavior and prediction models of unbound permeable aggregate base materials derived from tunneling rock wastes, *Materials*, **15**, 6005

23. WU C., WANG H., ZHAO J., JIANG X., YANJUN Q., YUSUPOV B., 2020, Prediction of viscoelastic pavement responses under moving load and nonuniform tire contact stresses using 2.5-D finite element method, *Mathematical Problems in Engineering*, 1029089

24. YAN M., WANG J., 2016, *Application of ABAQUS Finite Element Software in Pavement Structure Analysis*, Zhejiang University Press